Probe vehicle-based traffic state estimation method with spacing information and conservation law*

Toru Seo[†‡] Takahiko Kusakabe[†]

May 27, 2015

Abstract

This paper proposes a method of estimating a traffic state based on probe vehicle data that contain spacing and position of probe vehicles. The probe vehicles were assumed to observe spacing by utilizing an advanced driver assistance system, that has been implemented in practice and is expected to spread in the near future. The proposed method relies on the conservation law of the traffic flow but is independent of a fundamental diagram. The conservation law is utilized for reasonable aggregation of the spacing data to acquire the traffic state, i.e., a flow, density and speed. Its independence from a fundamental diagram means that the proposed method does not require predetermined nor exogenous assumptions with regard to the traffic flow model parameters. The proposed method was validated through a simulation experiment under ideal conditions and a field experiment conducted under actual traffic conditions; and empirical characteristics of the proposed method were investigated.

Keywords: probe vehicle; traffic flow; traffic state estimation; conservation law; spacing measurement; advanced driver assistance system

1 Introduction

Probe vehicles are one of the most effective methods for collecting road traffic data because of their wide coverage area over time and space. In particular, probe vehicles equipped with global positioning system (GPS) that report their position and speed are commonly used at present (e.g., Herrera et al., 2010).

Traffic states are represented by the flow, density and speed. These variables can be estimated by using partially observed traffic data. This is known as traffic state estimation (TSE) and has been incorporated with GPS-equipped probe vehicles (e.g., Nanthawichit et al., 2003; Herrera and Bayen, 2010; Yuan et al., 2012; Mehran et al., 2012). In order to estimate the states, traffic flow models such as the Lighthill–Whitham–Richards (LWR) model (Lighthill and Whitham, 1955; Richards, 1956) and its successors have often been assumed and utilized. The LWR model is based on two assumptions: the fundamental diagram (FD; also known as flow–density relationship) and the conservation law (CL). The FD has a significant role in probe vehicle-based TSEs with regard to acquiring the flow or density from the observed speed. Most existing TSE methods assume some exogenous conditions on an FD (e.g., its functional form and parameters). However, an FD is a complicated phenomenon that involves various factors (e.g., road and user characteristics) and cannot be described or predicted completely. Therefore, such exogenous assumptions for an FD may negatively affect the estimation robustness. On the other hand, the CL should always be satisfied in the estimation model except at merging/diverging positions. Our interest is the TSE by using probe vehicle data without a predetermined FD. This requires, however, additional observed data.

Recently, several technologies have been developed for acquiring information on the surrounding environment from a running vehicle. While their original and current purposes are for advanced driver assistance systems (ADASs), such as adaptive cruise control and autonomous driving (National Highway Traffic Safety Administration, 2013), they are also valuable for TSE because the spacing and speed of the vehicle must be measured precisely in order to enable effective ADAS. Seo et al. (2015) proposed a TSE method that simply aggregates such probe vehicle data to estimate flow and density. One of the deficiencies of Seo et al. (2015)'s method is its independence from traffic dynamics. For more sophisticated and precise estimation, traffic flow models need to be explicitly considered. The problem is that

*Manuscript published in *Transportation Research Part C: Emerging Technologies* 59, 391–403, 2015, doi:10.1016/j.trc.2015.05.019

[†]corresponding author. Email: t.seo@plan.cv.titech.ac.jp, Tel.: +81 3 5734 2575.

[‡]Transport Studies Unit, Tokyo Institute of Technology, 2-12-1-M1-20, O-okayama, Meguro, Tokyo 152-8552, Japan

almost all existing traffic flow models utilize an exogenously given FD, even though the FD can be directly observed by ADAS-equipped probe vehicles.

The objective of this study was to develop and validate a method that estimates the traffic state based on the observed spacing and position data of probe vehicles by considering the traffic dynamics. The proposed method utilizes a CL to represent the traffic dynamics. On the other hand, it does not use an explicit FD in order to eliminate exogenous factors. The developed method was verified by using actual data taken from a field experiment performed on an urban expressway as well as synthetic data generated by simulation. Section 2 describes the development of the proposed method. Section 3 and 4 describe its validation.

2 Estimation method

This section describes the proposed method of estimating traffic states based on observed spacing and position data from probe vehicles.

2.1 Concepts

The proposed method estimates traffic states in a road section where some of the vehicles in the traffic are probes that measure the geographic position and spacing of the vehicle ahead without any errors. The road section's schematics are assumed to be known to analysts. The probe vehicles' driving behavior is assumed to be the same as that of non-probe vehicles, i.e., the probes are randomly sampled from all of the vehicles. In addition, the traffic is assumed to be single-lane traffic that satisfies the first-in first-out (FIFO) condition in order to simplify the situation.

The spacing observed by a vehicle at a point depends on microscopic vehicular phenomena that depend on macroscopic traffic flow phenomena. For example, the spacing of a vehicle takes a volatile value that is often determined by whether the vehicle is the leader of a platoon or not; meanwhile, the formation of the platoon is mainly determined by the global traffic state. Therefore, aggregation is needed in order to estimate the global traffic state from the observed vehicular variables. In this method, the observed vehicular variables are aggregated based on the CL. Specifically, the number of vehicles between two specific probe vehicles is a constant along a section where merging/diverging positions (i.e., nodes in a road network) do not exist. This number of vehicles is estimated by aggregating the data observed by the two boundary probe vehicles. The estimation procedure is as follows: +2

Step 1 The number of vehicles between two consecutive probe vehicles and two consecutive merging/diverging positions is estimated based on the observed data of the two probe vehicles.

Step 2 The cumulative counts at the probe vehicle trajectories are calculated from the estimated number of vehicles.

Step 3 The continuous cumulative count over the entire time–space region is estimated by interpolating the cumulative counts at the probe vehicle trajectories.

Step 4 Traffic states (i.e., flow, density and speed) are derived by partially differentiating the continuous cumulative count.

Figure 1 visualizes the relationships between the cumulative count, vehicle trajectory, and traffic state (for details, see Makigami et al., 1971; Daganzo, 1997). The proposed method can be regarded as based on rectangles on the n–x coordinate plane, which is similar to the n–t Lagrangian coordinates of Leclercq et al. (2007); van Wageningen-Kessels et al. (2013) and is identical to coordinates of T-model by Laval and Leclercq (2013), because the primary subject of estimation is the number of vehicles in the n–x rectangles. Steps 1 and 2 are described in section 2.2; and steps 3 and 4 are described in section 2.3.

2.2 Estimation method for cumulative count at probe vehicle's trajectory

Consider the time–space region $\mathbf{A}_m^j$ surrounded by the

- trajectory of the m-th probe vehicle,
- trajectory of the leading vehicle of the $(m-1)$-th probe vehicle,
- the j-th merging/diverging position, and
- the $(j+1)$-th merging/diverging position.

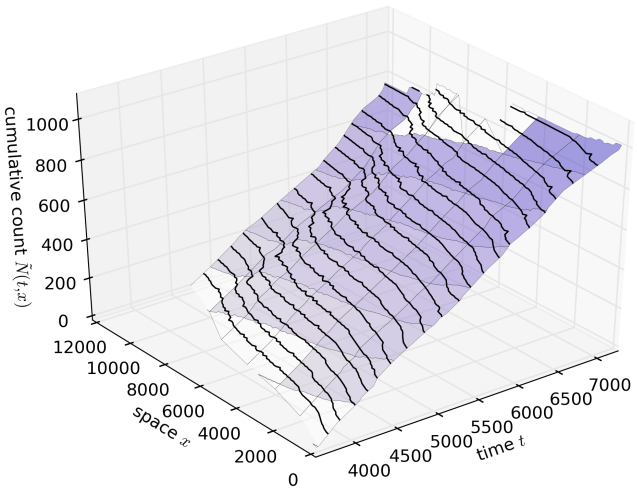

Figure 1: Three-dimensional representation of traffic flow. The height is the continuous cumulative count $\tilde{N}$, the contour line of $\tilde{N}$ is a vehicle's trajectory, the slope of $\tilde{N}$ in the t direction ($\partial\tilde{N}/\partial t$) is the flow q, and the slope of $\tilde{N}$ in the $-x$ direction ($-\partial\tilde{N}/\partial x$) is the density k.

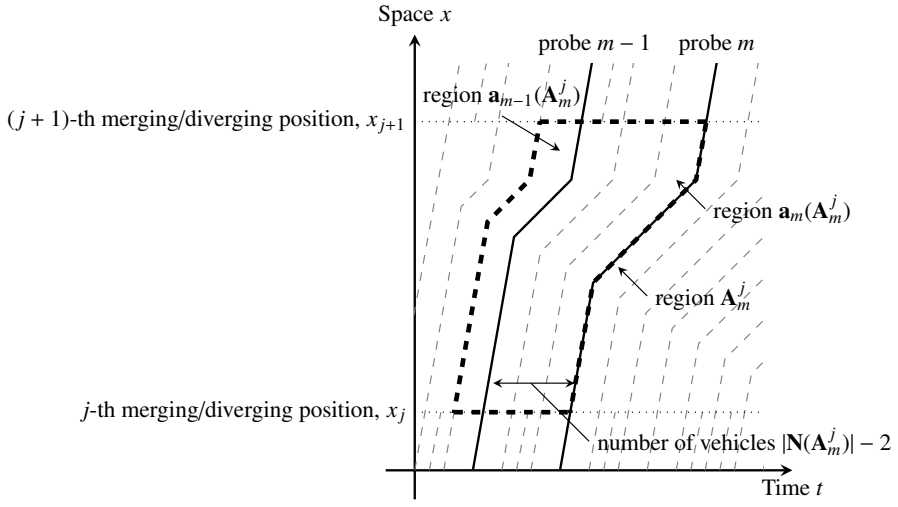

Figure 2: Method conceptualized as time–space diagram.

Figure 2 shows an example of region $\mathbf{A}_m^j$. Because of this definition and the FIFO assumption, the number of vehicles in the region $\mathbf{A}_m^j$ is always identical to the number of vehicles between the m-th probe vehicle and the leading vehicle of the $(m-1)$-th probe vehicle. The following notations are employed to represent the time and space coordinates: x_m^t is the position of the m-th probe vehicle at the time point t, t_m^x is the time point of the m-th probe vehicle at the position x, and x_j is the position of the j-th merging/diverging position.

The cumulative count $N(t,x)$ at a probe vehicle's trajectory—with the 0th probe vehicle[1]as a reference point—is described by using the number of vehicles between two probe vehicles as follows:

$$N(t_0^x, x) = 0, \tag{1a}$$

$$N(t_m^x, x) = N(t_{m-1}^x, x) + |\mathbf{N}(\mathbf{A}_m^j)| - 2 \qquad (m \geq 1,\ x_j < x < x_{j+1}), \tag{1b}$$

where $\mathbf{N}(\mathbf{A})$ is the set of all vehicles in the time–space region $\mathbf{A}$ and $|\mathbf{N}(\mathbf{A})|$ is the number of vehicles of $\mathbf{N}(\mathbf{A})$. Equation (1) means that the number of vehicles between the m-th and $(m-1)$-th probe vehicles at the position x (i.e., $N(t_m^x, x) - N(t_{m-1}^x, x)$) is identical to the number of vehicles in the region $\mathbf{N}(\mathbf{A}_m^j)$ minus two[2] (i.e., $|\mathbf{N}(\mathbf{A}_m^j)| - 2$) if the position x is between the j-th and $(j+1)$-th merging/diverging positions.

The only unknown variable in (1) is $\mathbf{N}(\mathbf{A}_m^j)$. This can be estimated from the probe vehicle data as follows:

$$|\hat{\mathbf{N}}(\mathbf{A}_m^j)| = \frac{|\mathbf{A}_m^j|}{\left(|\mathbf{a}_{m-1}(\mathbf{A}_m^j)| + |\mathbf{a}_m(\mathbf{A}_m^j)|\right)/2}, \tag{2}$$

where $\mathbf{a}_m(\mathbf{A})$ is the time–space region between the m-th probe vehicle and its leading vehicle in region $\mathbf{A}$, which should be observed by the probe vehicle, and $|\mathbf{A}|$ is the area of the region $\mathbf{A}$. Equation (2) means that all vehicles in time–space region $\mathbf{A}_m^j$ are distributed with a time–space interval of $(|\mathbf{a}_{m-1}(\mathbf{A}_m^j)| + |\mathbf{a}_m(\mathbf{A}_m^j)|)/2$, which is the average of the two probe vehicle's intervals. This is consistent with the generalized definitions of Edie (1963). It also implies that the number of vehicles between two vehicles is determined by the two vehicles' spacing at a road section without merging/diverging positions. By using the estimated value, the cumulative count at a probe vehicle's trajectory (1) can be calculated as follows:

$$\hat{N}(t_0^x, x) = 0, \tag{3a}$$

$$\hat{N}(t_m^x, x) = \hat{N}(t_{m-1}^x, x) + |\hat{\mathbf{N}}(\mathbf{A}_m^j)| - 2 \qquad (m \geq 1,\ x_j < x < x_{j+1}). \tag{3b}$$

2.3 Estimation method for traffic state

The flow, which is defined as $q = \partial\tilde{N}/\partial t$, can be estimated as

$$\hat{q}(t,x) = \frac{\hat{N}(t_m^x, x) - \hat{N}(t_{m-1}^x, x)}{t_m^x - t_{m-1}^x} \qquad (t_{m-1}^x < t \leq t_m^x). \tag{4}$$

The continuous cumulative count $\tilde{N}$ is estimated from

$$\hat{\tilde{N}}(t,x) = \int_{t_0^x}^{t} \hat{q}(\tau, x)\mathrm{d}\tau. \tag{5}$$

In fact, (4) and (5) mean that $\hat{\tilde{N}}$ is linearly interpolated from the discrete $\hat{N}$ of (3) over the t-axis (Figure 3 (a)) where uniform distribution of the vehicles between t_m^x and t_{m-1}^x is assumed.

Once the continuous cumulative count is obtained, the density and speed can be estimated as

$$\hat{k}(t,x) = -\frac{\partial\hat{\tilde{N}}(t,x)}{\partial x}, \tag{6}$$

$$\hat{v}(t,x) = \frac{\hat{q}(t,x)}{\hat{k}(t,x)}, \tag{7}$$

[1]This vehicle is to be specified by an analyst

[2]the $(m-1)$-th probe vehicle and its leading vehicle

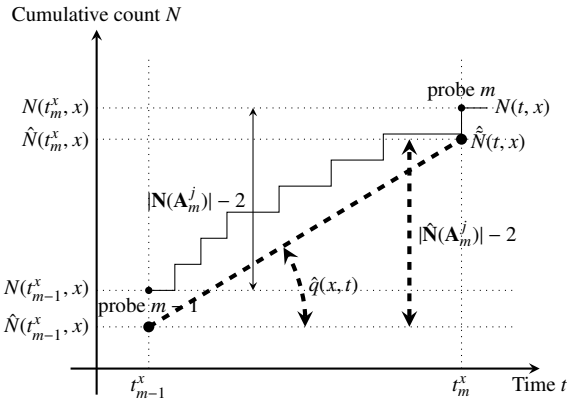

(a) n–t cumulative curve at certain point x in space (x_j, x_{j+1}).

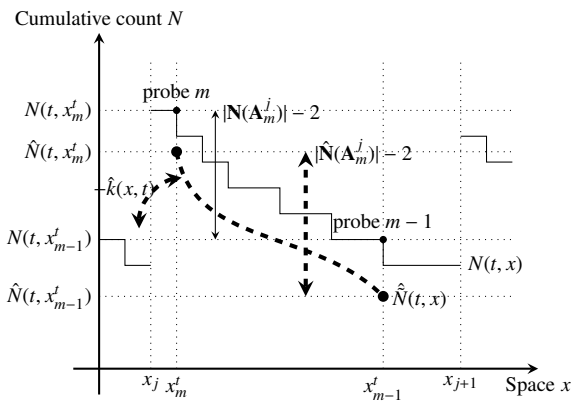

(b) n–x cumulative curve at certain time point t where $x_j \leq x_m^t < x_{m-1}^t \leq x_{j+1}$ is satisfied.

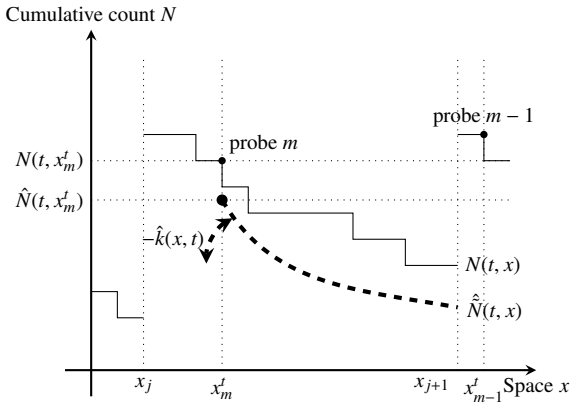

(c) n–x cumulative curve at certain time point t where $x_j \leq x_m^t < x_{j+1} < x_{m-1}^t$ is satisfied.

Figure 3: Illustrated examples of estimation method on cumulative curves.

based on their definitions, namely, $k = -\partial\tilde{N}/\partial x$ and $v = q/k$, except at the merging/diverging positions.

The estimation procedure can also be visualized as shown in Figure 3. First, the number of vehicles between two convective probe vehicles $|\hat{\mathbf{N}}(\mathbf{A}_m^j)|-2$ is estimated based on the observed data from probe vehicles. Then, the cumulative count $\hat{N}(t_{m-1}^x, x)$, $\hat{N}(t_m^x, x)$ and continuous cumulative count $\hat{\hat{N}}(t, x)$ are estimated along with the cumulative count's slope on the n–t plane, which means the flow $\hat{q}(x, t)$ between t_{m-1}^x and t_m^x, as shown in Figure 3(a). By using the continuous cumulative count $\hat{\hat{N}}(t, x)$, the density $\hat{k}(x, t)$ can be estimated as the slope of $\hat{\hat{N}}(t, x)$ on the n–x plane, as shown in Figure 3(b) and (c).

2.4 Discussions on the proposed method

The proposed method can derive the flow, density, and speed without an explicit FD, meaning that no exogenous assumptions on an FD. Therefore, the proposed method can easily be applied to various traffic conditions, especially when an FD is unknown or unpredictable. Its independence from an FD also means that the proposed method can be utilized to estimate the FD itself. In fact, estimating the cumulative count based on (2) is identical to estimating the area-flow (c.f., MFD; Geroliminis and Daganzo, 2008; Daganzo and Geroliminis, 2008) between two merging/diverging positions and two consecutive probe vehicles. It implies that if a well-defined MFD exist in the region (Daganzo and Geroliminis (2008) prove this fact under certain conditions such as a link with constant FD), the proposed method could be accurate.

The proposed method utilizes the CL in order to estimate the traffic state from vehicles' spacing. This means that the traffic state of a certain time point and position is estimated based on spacings observed by the same vehicle over a wider area of time and space. Therefore, the precision of the estimated traffic state is relatively robust against fluctuations in

microscopic vehicular phenomena (e.g., vehicle platoons, lane-changing) comparing to the estimation method proposed by Seo et al. (2015) that does not consider the CL. As noted earlier, equation (2) is identical to estimating the area-flow from the probe vehicle data based on Edie's generalized definition. Therefore, the accuracy and precision of $|\hat{\mathbf{N}}(\mathbf{A}_m^j)|$ can be analytically approximated based on the results of Seo et al. (2015), as follows:

$$E\left[|\hat{\mathbf{N}}(\mathbf{A}_m^j)|\right] - |\mathbf{N}(\mathbf{A}_m^j)| \simeq \frac{|\mathbf{A}_m^j|\,\sigma\left(\bar{h}_n(\mathbf{A}_m^j)\right)^2}{2(x_{j+1}-x_j)\mu\left(\bar{h}_n(\mathbf{A}_m^j)\right)^3}, \tag{8}$$

$$\text{RMSE}\left(|\hat{\mathbf{N}}(\mathbf{A}_m^j)|\right) \simeq \frac{|\mathbf{A}_m^j|}{(x_{j+1}-x_j)\mu\left(\bar{h}_n(\mathbf{A}_m^j)\right)^2}\sqrt{\frac{\sigma\left(\bar{h}_n(\mathbf{A}_m^j)\right)^2}{2}}, \tag{9}$$

where $\mu()$ represents the mean, $\sigma()^2$ represents the variance, $\bar{h}_n(\mathbf{A}_m^j)$ represents the mean headway of a vehicle n in the region $\mathbf{A}_m^j$, and RMSE is root mean square error and taken as an index for precision. Equations (8) and (9) mean that the accuracy and precision of the estimated cumulative count N are improved as mean of the vehicle's mean headways increases and the variance of the vehicle's mean headways decreases. Therefore, the accuracy and precision of the estimated traffic state have similar tendencies.

By using examples, following explains expected behavior of the vehicle's mean headways, $\sigma(\bar{h}_n(\mathbf{A}))^2$, and its relation to the errors of the proposed method. Consider following situation: vehicles are traveling through a long link; their desired-speeds are varied; and the traffic is under free flow state. If a platoon formed by the vehicles is kept continuously during traveling through the link (e.g., a platoon enters a link, then exits from the link without vehicles addition nor removing), the headway variance becomes large. In this case, large estimation error will be expected; and it can be regarded as a limitation of the proposed method. On the other hand, if the vehicles are newly forming and/or declining a platoon during traveling through the link (e.g., vehicles randomly enter a link, then form a platoon in the middle of the link), the variance will be smaller. In this case, the error will be smaller than the first case. This improvement is the positive effect due to incorporating a CL. The spacing-based method without considering a CL of Seo et al. (2015) estimates a traffic state in a short road segment using data collected from the segment itself; so, estimation error can be large because vehicles may keep a platoon formed in the segment. In contrast, the proposed method in this paper estimates a traffic state in a position using data collected from the entire link; so, estimation error can be smaller because platoons may be newly formed and/or declined in the link.

The deficiencies of the proposed method are as follows. First, single-lane traffic and FIFO condition were assumed in order to estimate the number of vehicles between two probe vehicles; such assumptions are not always satisfied in the real world. However, the proposed method can be applied to traffic where these conditions are not satisfied if the probe vehicle's driving behavior is the same as other vehicles. This is because the expected number of vehicles that overtake a probe vehicle and number that are overtaken by a probe vehicle is equal to each other. In addition, estimation error may sometimes decrease under non-FIFO condition; because a platoon will be formed and/or declined frequently under such condition. Note that if the road has multiple lanes, the cumulative number (3) needs to be multiplied by the number of lanes. Second, the linear interpolation of the cumulative count over time is limited in its ability to reproduce shockwaves. Another deficiency is that real-time states cannot be estimated. Therefore, short-term future prediction is required in order to obtain the real-time states[3].

3 Simulation experiment-based validation of proposed method

This section presents the validation of the proposed method though a simulation experiment. First, section 3.1 summarizes the conditions of the field experiment. Section 3.2 describes the estimation results. Section 3.3 investigates the effect of incorporating the CL.

3.1 Simulation scenario

A microscopic traffic flow simulator called AIMSUN, which was developed by TSS-Transport Simulation Systems, was employed for the simulation. The simulator generates traffic data based on the car-following model developed by Gipps (1981). The road section in the simulation had a single-lane and length of 5 km with homogeneous geometry except for a

[3]This prediction can be based on the estimated traffic state and an FD that can be estimated with the proposed method.

Table 1: Vehicle behavior parameter setting in simulation.

Parameter name	Mean	Deviation
Desired speed (km/h)	80	10.0
Max acceleration (m/s^2)	3	0.2
Normal deceleration (m/s^2)	4	0.25
Max deceleration (m/s^2)	6	0.5
Min spacing (m)	1	0.3
Vehicle length (m)	4	0.5

Table 2: Error indices for scenarios with proposed method.

Probe vehicle penetration rate	Flow (veh/h)		Density (veh/km)		Speed (km/h)	
P	RMSPE($\hat{q}$)	Bias($\hat{q}$)	RMSPE($\hat{k}$)	Bias($\hat{k}$)	RMSPE($\hat{v}$)	Bias($\hat{v}$)
0.2%	59%	151.0	107%	-1.6	134%	1.1
1.0%	55%	134.8	87%	2.2	61%	-2.1
3.5%	42%	83.6	52%	2.1	36%	-0.7
5.0%	38%	69.6	48%	2.4	36%	-0.2
10.0%	33%	63.8	45%	2.4	38%	0.7

bottleneck at the end of the section. Note that this road setting always satisfies the assumptions in the proposed method[4]. The vehicles in the simulation had heterogeneous driving behaviors, such as the desired speed. Table 1 summarizes the parameters. The probe vehicles were randomly sampled from all the vehicles to simulate a given penetration rate. Note that the proposed method does not utilize information on a penetration rate. The position and spacing data of the probe vehicles with 1 s interval were used for estimating traffic states.

A traffic situation with a queue was generated using simulation, by setting the demand from upstream of the section and the capacity at the bottleneck at the end of the section. Ground truth states was available because this was a simulation experiment. Figure 4(a)–(d) shows the ground truth states (flow q, density k, speed v) and cumulative count $\tilde{N}$ as time–space diagrams. By applying the proposed method to the generated traffic situation, the characteristics of the proposed method in various traffic situations (e.g., free flow, congested flow, flow with backward wave and flow with forward wave) can be investigated.

3.2 Results of traffic state estimation

The estimated variables were the traffic states at certain time–space resolutions (i.e., the intervals for the central differences) and the cumulative count in the section. The cumulative count was calculated at 1 min time intervals and 100 m space intervals according to (5). The density $\hat{k}$ was calculated based on the central differences at 100 m intervals according to (6).

Figure 4(e)–(h) shows the estimated traffic state $(\hat{q}, \hat{k}, \hat{v})$ and cumulative count $\hat{\tilde{N}}$ as time–space diagrams where the probe vehicle penetration rate is 3.5%. Through comparison with the ground truth shown in Figure 4(a)–(d), the estimation can be used to acquire tendencies of the actual traffic, such as the queue propagation and dissolution. More detailed phenomena such as stop-and-go waves were partially captured with some errors. The errors were due to a deficiency of the method of interpolating the continuous cumulative count in the proposed methods, namely, liner interpolation over the time.

Figure 5 compares the estimated variables and ground truth as scatter diagrams. The estimated variables well corresponded at most of true states although the values were slightly overestimated, as suggested by the analytically expected bias in (9).

Table 2 summarizes the error indices of the TSE for different combinations of the probe vehicle penetration rate P. The RMSPE and bias were employed as error indices, which are defined as RMSPE$(\hat{\theta}) = \sqrt{E[((\hat{\theta}-\theta)/\theta)^2]}$ and Bias$(\hat{\theta}) = E[\hat{\theta}-\theta]$, respectively. The error indices of each scenario were calculated from 100 iterations under different samplings of probe vehicles. The results showed clear improvements in the estimation accuracy and precision as the penetration rate was increased. Almost all of the scenarios overestimated the states similar to Figure 5(d) and for the same reason.

[4]Except the first vehicle enters the road; because it does not have its leader. We removed it from candidates for the probe vehicles.

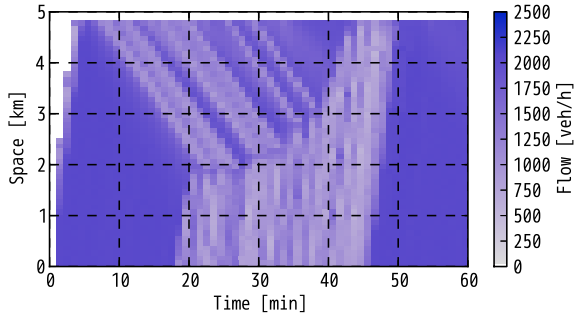

(a) Ground truth flow q.

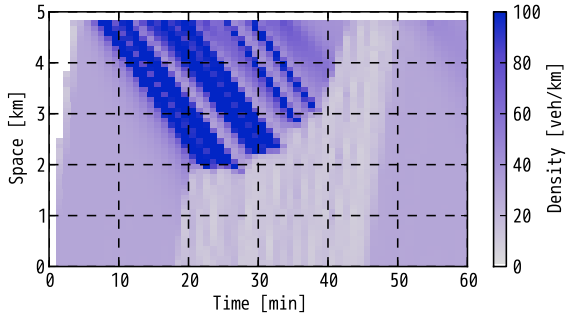

(b) Ground truth density k.

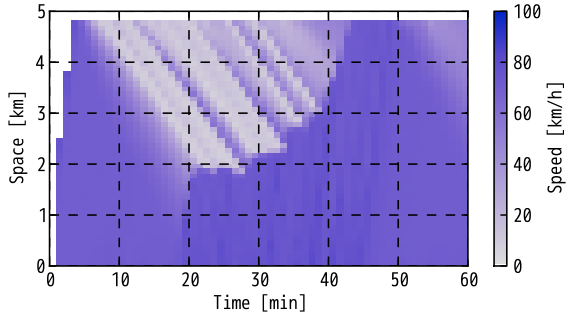

(c) Ground truth speed v.

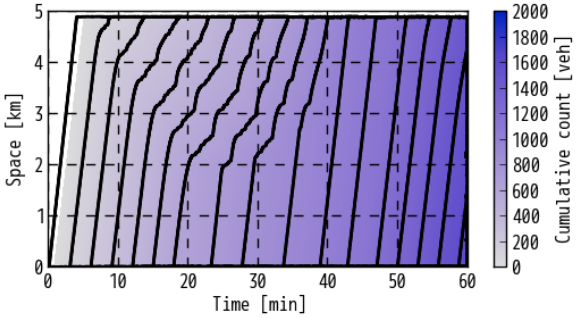

(d) Ground truth cumulative count $\tilde{N}$. The contour lines were drawn at intervals of 100 veh.

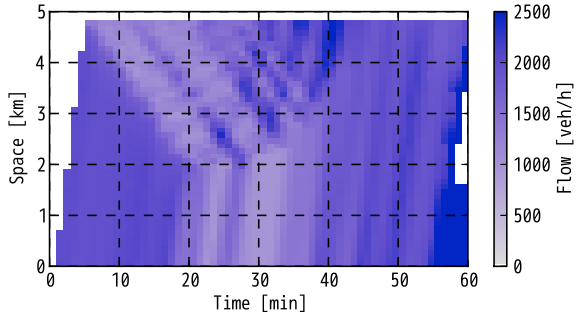

(e) Flow $\hat{q}$ estimated with proposed method.

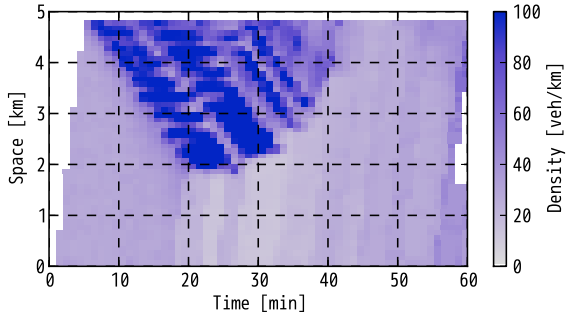

(f) Density $\hat{k}$ estimated with proposed method.

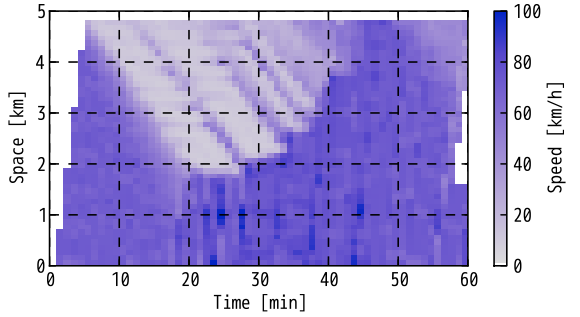

(g) Speed $\hat{v}$ estimated with proposed method.

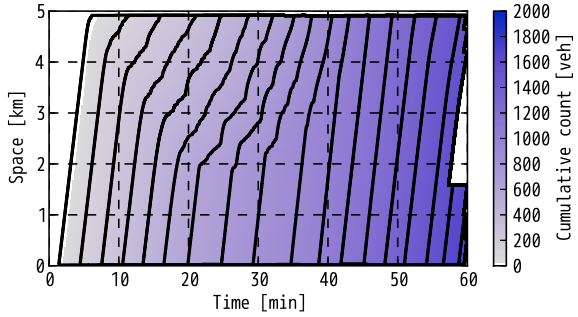

(h) Cumulative count $\hat{\tilde{N}}$ estimated with proposed method. The contour lines were drawn at intervals of 100 veh.

Figure 4: Time–space diagrams of traffic state and cumulative count.

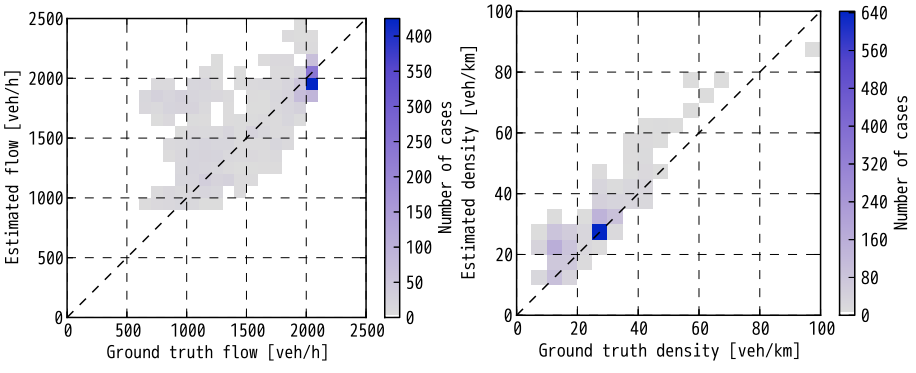

(a) Flow q.

(b) Density k.

(c) Speed v.

(d) Cumulative count $\tilde{N}$.

Figure 5: Scatter diagrams of estimated variables vs. ground truth variables.

Table 3: Comparison between proposed method and method of Seo et al. (2015).

P	RMSPE($\hat{q}$)	RMSPE($\hat{q}_{\text{withoutCL}}$)	PoI
0.2%	59%	66%	12%
1.0%	55%	63%	7%
3.5%	42%	59%	27%
5.0%	38%	53%	38%
10.0%	33%	52%	43%

3.3 Effect of incorporating CL

In order to investigate the effect of incorporating the CL, the flow was estimated using the method proposed by Seo et al. (2015) which does not consider the CL but uses the same probe vehicle data. The estimated flow using this method was defined as $\hat{q}_{\text{withoutCL}}$ in this paper. The time and space resolution for calculating $\hat{q}_{\text{withoutCL}}$ were identical to the intervals of the central difference in the proposed method: 1 min and 100 m. Table 3 presents the comparison results. As an index representing the positive effect of incorporating the CL, the percentage of improvement (PoI) is employed;it is defined as $(\text{RMSPE}(\hat{q}_{\text{withoutCL}}) - \text{RMSPE}(\hat{q}))/\text{RMSPE}(\hat{q})$. According to the results, incorporating the CL clearly improved the estimation precision, especially at high penetration rates.

4 Field experiment-based validation of proposed method

In order to investigate the applicability of the proposed method to the real world, the proposed method was validated by using data collected from a field experiment at an actual road.

4.1 Field experiment

A field experiment was conducted on September 24 (Tuesday), 2013, from 15:00 to 16:00 at an urban expressway in Tokyo. Only the minimum necessary information of the experiment is summarized here; a detailed description and evaluation of this experiment are provided in Seo et al. (2015).

The location was the Inner Circular Route (i.e., C1) of the Metropolitan Expressway, which is an urban expressway in Tokyo, Japan. Figure 6 shows the schematics of C1. The junction is abbreviated as JCT, the arrows on the upper side represent the merging/diverging section with other highway routes, and the arrows on the lower side represent on/off ramps. Most of C1 has two lanes, namely, cruising and passing lanes, with a speed limit of 50 km/h. Because of the presence of tunnels and law restrictions, the survey section was limited to an 11 km long section of the cruising lane, namely, from the 0 km point to the 11 km point in Figure 6. C1 was equipped with many detectors at 250 m intervals for each lane with time aggregation at 1 min intervals. The traffic state observed by these detectors was compared with that estimated by the proposed method. Figure 7(a)–(d) show the state (flow q, density k, speed v) observed by the detectors and cumulative count $\tilde{N}$ as time–space diagrams. The cumulative count was calculated from the flow observed by detectors with a probe vehicle's trajectory as a reference point. Discontinuities in the contour lines present junctions (merging/diverging sections from/to other highway routes) in C1; these are represented as arrows on the upper side in Figure 6. Note that the cumulative count $\tilde{N}$ did not always increase as t increased and x decreased when there were no merging/diverging. This is because of the on/off-ramps, lane-changing by vehicles, and systematic errors in the measurements of the detectors.

Twenty standard-size passenger vehicles equipped with GPS loggers and video cameras and driven by non-professional drivers were employed as probe vehicles. The positions of the probe vehicles were identified from the GPS log. The spacings from each probe vehicle to its leading vehicle were estimated by analyzing the size of the leading vehicle in images captured by the camera. Most of the probe vehicles drove three laps on C1 during the experiment period, and a total of 59 laps were performed in the survey section. This corresponded to 42.1 veh/h/lane. Therefore, the probe vehicle's penetration rate roughly corresponded to 3.5% according to the average flow of all of the vehicles (1255.2 veh/h/lane) observed by the detectors.

4.2 Validation results

The estimation targets were the traffic state at certain time and space resolutions and the cumulative count in the survey section. The cumulative count was calculated at 1 min time intervals and 100 m space intervals according to (5). The density $\hat{k}$ was calculated based on central differences at 100 m intervals according to (6). In order to compare the estimated

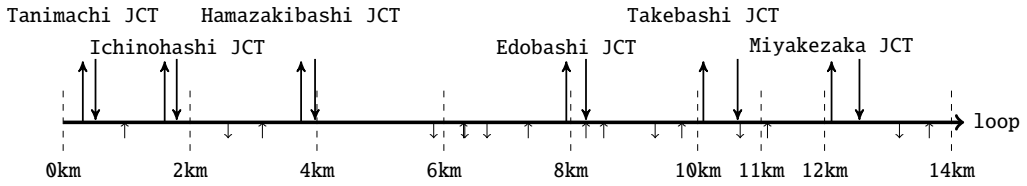

Figure 6: Schematic of experiment site: Inner Circular Route (counterclockwise direction).

Table 4: Error indices for scenarios with proposed method in field experiment.

Probe vehicle penetration rate	Flow (veh/h)		Density (veh/km)		Speed (km/h)	
P	RMSPE($\hat{q}$)	Bias($\hat{q}$)	RMSPE($\hat{k}$)	Bias($\hat{k}$)	RMSPE($\hat{v}$)	Bias($\hat{v}$)
0.2%	30%	-158.9	39%	-4.9	60%	0.9
3.5%	23%	-133.9	30%	-2.3	24%	-2.1

states with the detector data, the estimated states were averaged at a time resolution of 5 min and space resolution of 500 m. The proposed method requires the positions of the merging/diverging positions to be specified. In this estimation, only junctions were considered to be merging/diverging positions. Thus, on/off-ramps and lane-changing were ignored.

Figure 7(e)–(h) show the estimated traffic state $(\hat{q}, \hat{k}, \hat{v})$ with a 5 min $\times$ 500 m resolution and cumulative count $\hat{\tilde{N}}$ as a time–space diagram. Through a comparison with Figure 7(a)–(d), the estimation can be used to acquire the tendencies of the detectors' observed variables (e.g., a queue propagation from the 8 km point). Figure 8 compares the estimated variables and detectors' observed variables as scatter diagrams. According to the figures, the estimated variables well corresponded at most of detectors' observed states. However, the values tended to be underestimated. One of the reasons was a bias in the probe vehicles' driving behavior (i.e., their driving behaviors tended to be safer, which meant a slower speed and larger spacing than for other vehicles).

Table 4 summarizes the error indices of the TSE for different probe vehicle penetration rates P. The penetration rate of 0.2% was reproduced by randomly sampling all of the probe vehicles. This corresponded to roughly 2 probe veh/h. The error indices of scenarios with a 0.2% penetration rate were calculated from 25 iterations under different sampling conditions of the probe vehicles. According to the results, the estimation precision clearly increased with the penetration rate. Note that most of the scenarios underestimated the states, similar to Figure 8 and for the same reasons. Table 5 compares results of the proposed method and the method without considering the CL; the precision was improved with the proposed method.

4.3 Comparison between the simulation experiment and the field experiment based validations

Table 6 summarizes the difference between the simulation experiment (Section 3) and field experiment (Section 4). The simulation experiment was conducted under traffic conditions where the assumptions of the proposed method were always satisfied. On the other hand, the field experiment-based validation had some limitations, such as slight violations of the assumption. However, it allowed the proposed method's characteristics to be validated under actual traffic conditions. This advantage is important for validating the proposed method's practical characteristics because of the proposed method's strong dependence on the spacing, which was determined by a synthetic model (i.e., car-following model) in the simulation experiment.

The validation results suggest that the proposed method works well in an actual traffic environment, although the assumptions of the proposed method (i.e., the CL) were not exactly satisfied because of the on/off-ramps and lane-changing. For example, the precision increased with the penetration rate in both the simulation (Table 2) and field experiment (Table 4). In fact, the proposed method shwed better precision in the field experiment than in the simulation experiment. Ironically, one of the reasons is existence of lane-changing. They decrease the variance in the mean headway; then the estimation precision of the cumulative count improved (c.f., (9)).

Table 5: Comparison between results of field experiment with proposed method and method of Seo et al. (2015).

P	RMSPE($\hat{q}$)	RMSPE($\hat{q}_{\text{withoutCL}}$)	PoI
0.2%	30%	43%	30%
3.5%	23%	26%	13%

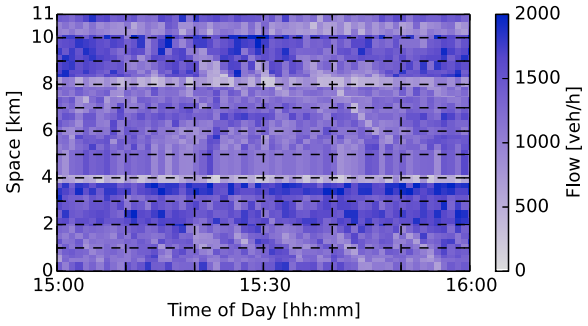

(a) Flow q observed by detectors.

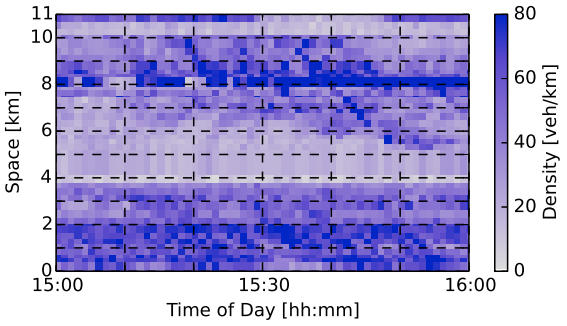

(b) Density k observed by detectors.

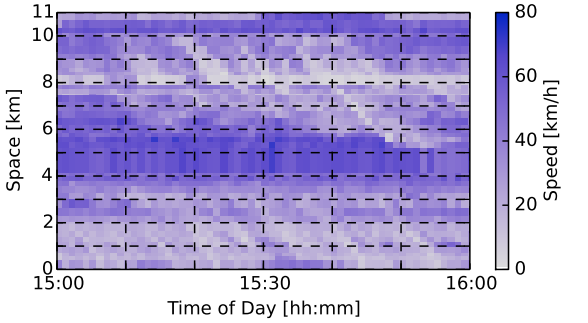

(c) Speed v observed by detectors.

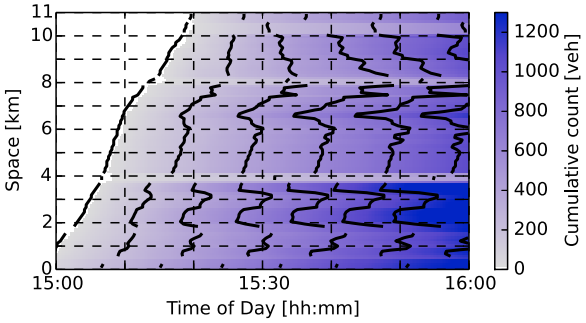

(d) Cumulative count $\tilde{N}$ observed by the detectors. The contour lines were drawn at intervals of 200 veh.

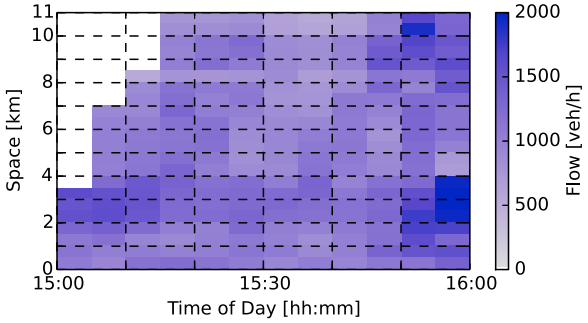

(e) Flow $\hat{q}$ estimated with proposed method.

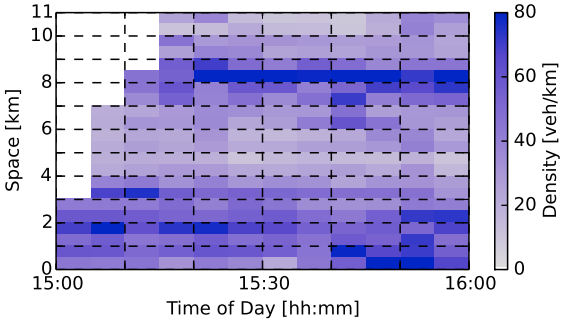

(f) Density $\hat{k}$ estimated with proposed method.

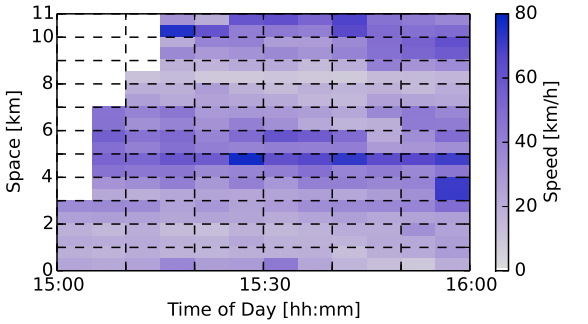

(g) Speed $\hat{v}$ estimated with proposed method.

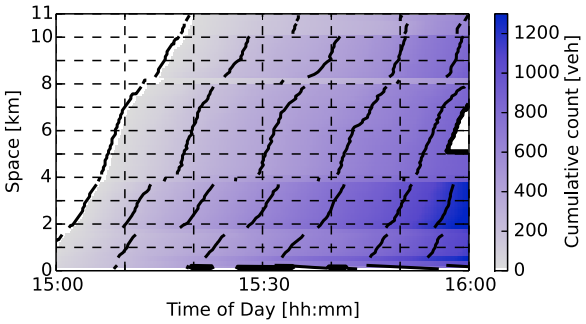

(h) Cumulative count $\hat{\tilde{N}}$ estimated with proposed method. The contour lines were drawn at intervals of 200 veh.

Figure 7: Time–space diagrams of traffic state and cumulative count in field experiment.

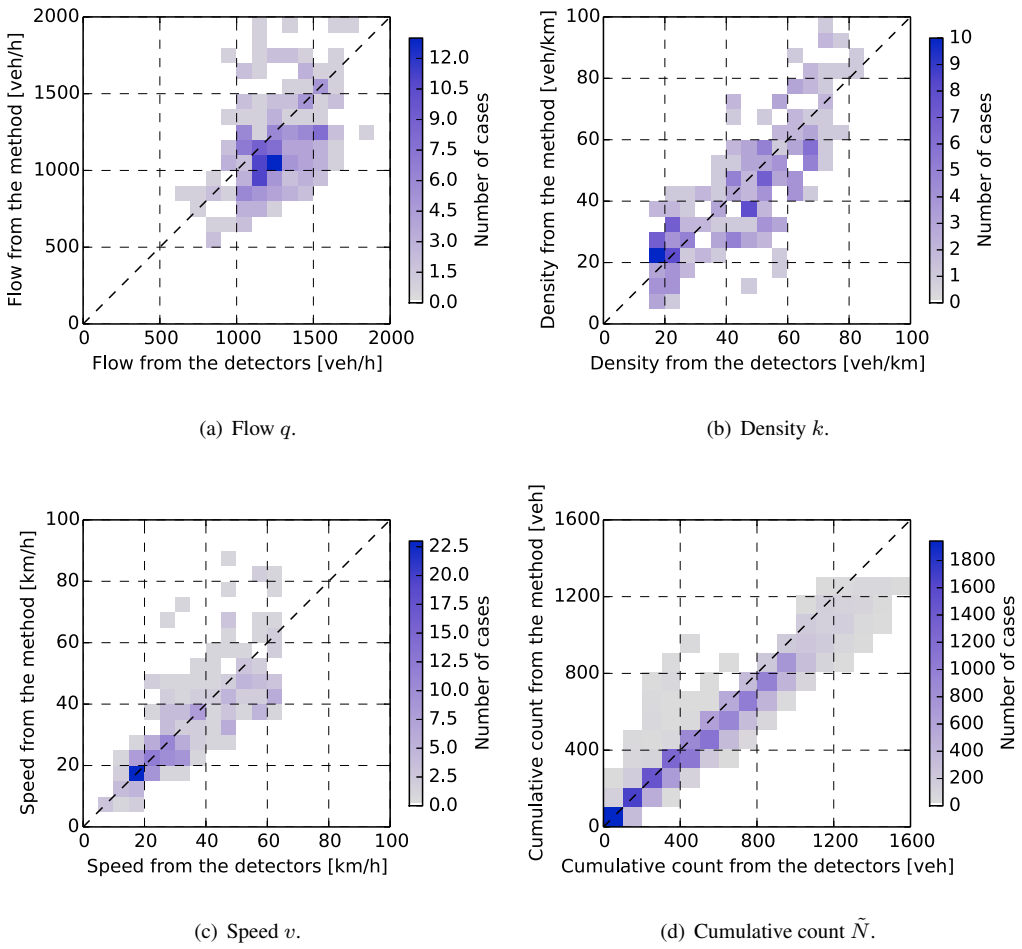

(a) Flow q.

(b) Density k.

(c) Speed v.

(d) Cumulative count $\tilde{N}$.

Figure 8: Scatter diagrams of estimated variables vs. detectors' observed variables in field experiment.

Table 6: Difference between validations based on simulation experiment and field experiment.

	The simulation experiment	The field experiment
FIFO condition	Always satisfied	Not always satisfied
CL	Always satisfied	Not always satisfied
Traffic flow model	Car-following model of Gipps (1981)	Actual traffic
Traffic condition	Synthetic scenario	Actual traffic
Driving behavior of probe vehicles	Not biased	Slightly biased
Ground truth	Available	Detectors
RMSPE($\hat{q}$) at P=0.2%	59%	30%
RMSPE($\hat{q}$) at P=3.5%	42%	23%
Bias($\hat{q}$) at P=0.2%	151.0 veh/h	-158.9 veh/h
Bias($\hat{q}$) at P=3.5%	83.6 veh/h	-133.9 veh/h
PoI due to incorporating CL at P=0.2%	12%	30%
PoI due to incorporating CL at P=3.5%	27%	13%

The notable difference between the two validation is a sign of the biases. The simulation-based validation (Table 2) and analytical approximation (8) showed positive biases, while the field experiment-based validation showed negative biases. This may be due to biases in the probe vehicles' driving behaviors. The probe vehicles tended to be slower than other vehicles, according comparison between the probe vehicle's speed and traffic speed observed by detectors.

Incorporating the CL improved the precision in both validations (Tables 3 and 5). However, in the field experiment scenario, the PoI decreased as the penetration rate was increased; this tendency was the inverse of that in the simulation-based validation. This may be due to violations of the assumptions. If a large amount of probe vehicle data is available (i.e., the traffic state can be estimated precisely even without the CL being incorporated) the non-exact assumptions of the CL will negatively affect the precision.

5 Conclusion

This paper proposes a TSE method that depends on probe vehicle data only, when probe vehicles can observe their spacing and position. In order to estimate the flow and density from the probe vehicle's spacing, an aggregation method based on a CL is developed. The proposed method is based on using rectangles on the n–x coordinate plane instead of the traditional x–t Eulerian coordinates or n–t Lagrangian coordinates. The proposed method does not consider or assume an FD, which is the other fundamental principle of a traffic flow model. Therefore, the proposed method does not require predetermined nor exogenous assumptions for an FD. This makes the proposed method widely applicable to any traffic situation and robust against sudden changes in a traffic situation, such as an accident.

The proposed method was validated using probe vehicle data that were acquired from a simulation experiment and a field experiment. The simulation experiment was performed under ideal condition that the assumptions of the proposed method were always satisfied, while the field experiment was not. The results from both synthetic and actual traffic data suggested that the proposed method is capable of estimating the traffic state relatively precise compared to the previous study. In particular, incorporating the CL clearly improved the estimation precision.

Several improvements can be suggested for future studies. First, an advanced estimation method for a continuous cumulative count derived from the discrete cumulative count at the probe vehicle trajectories is required. The estimation was treated by a linear interpolation over time ((4) and (5)) in this study. This caused some deficiencies in reproducing detailed traffic phenomena, such as shockwaves. We are currently developing a method of detecting shockwaves from the probe vehicle data and a method for linear interpolation of the cumulative count over shockwaves. Second, incorporating an endogenous estimation of an FD is another option to estimate the continuous cumulative count. Because the probe vehicle data contain spacing and time headway, an FD can be endogenously estimated. Then, vehicle trajectory estimation methods based on a traffic flow model with an FD and initial/boundary conditions (e.g., Laval and Leclercq, 2013) can be utilized for estimation. Combined with the second point (i.e., endogenous shockwave detection), this methodology will be also valuable for empirical investigations on traffic theory because traffic dynamics can change significantly when shockwaves pass through (Laval, 2011). Third, the CL at nodes should be considered. If probe vehicles are spread over a road network, the CL at nodes can be explicitly described because of the presence of probe vehicles at all links. This will solve the problem of neglecting the flow of the on/off-ramps.

Acknowledgments

The traffic detector data were kindly provided by Metropolitan Expressway Co., Ltd. We thank anonymous reviewers for their insightful comments on this paper including the title. Part of this work was financially supported by the Research Fellow DC2 program of the Japan Society for the Promotion of Science (KAKENHI Grant-in-Aid for JSPS Fellows #26010218).

References

Daganzo, C.F., 1997. Fundamentals of Transportation and Traffic Operations. Pergamon Oxford.

Daganzo, C.F., Geroliminis, N., 2008. An analytical approximation for the macroscopic fundamental diagram of urban traffic. Transportation Research Part B: Methodological 42, 771–781.

Edie, L.C., 1963. Discussion of traffic stream measurements and definitions, in: Almond, J. (Ed.), Proceedings of the 2nd International Symposium on the Theory of Traffic Flow, pp. 139–154.

Geroliminis, N., Daganzo, C.F., 2008. Existence of urban-scale macroscopic fundamental diagrams: Some experimental findings. Transportation Research Part B: Methodological 42, 759–770.

Gipps, P.G., 1981. A behavioural car-following model for computer simulation. Transportation Research Part B: Methodological 15, 105–111.

Herrera, J.C., Bayen, A.M., 2010. Incorporation of Lagrangian measurements in freeway traffic state estimation. Transportation Research Part B: Methodological 44, 460–481.

Herrera, J.C., Work, D.B., Herring, R., Ban, X.J., Jacobson, Q., Bayen, A.M., 2010. Evaluation of traffic data obtained via GPS-enabled mobile phones: The Mobile Century field experiment. Transportation Research Part C: Emerging Technologies 18, 568–583.

Laval, J.A., 2011. Hysteresis in traffic flow revisited: An improved measurement method. Transportation Research Part B: Methodological 45, 385–391.

Laval, J.A., Leclercq, L., 2013. The Hamilton–Jacobi partial differential equation and the three representations of traffic flow. Transportation Research Part B: Methodological 52, 17–30.

Leclercq, L., Laval, J.A., Chevallier, E., 2007. The Lagrangian coordinates and what it means for first order traffic flow models, in: Allsop, R., Bell, M., Heydecker, B. (Eds.), Transportation and Traffic Theory 2007, Elsevier. pp. 735–753.

Lighthill, M.J., Whitham, G.B., 1955. On kinematic waves. II. a theory of traffic flow on long crowded roads. Proceedings of the Royal Society of London. Series A. Mathematical and Physical Sciences 229, 317–345.

Makigami, Y., Newell, G.F., Rothery, R., 1971. Three-dimensional representation of traffic flow. Transportation Science 5, 302–313.

Mehran, B., Kuwahara, M., Naznin, F., 2012. Implementing kinematic wave theory to reconstruct vehicle trajectories from fixed and probe sensor data. Transportation Research Part C: Emerging Technologies 20, 144–163.

Nanthawichit, C., Nakatsuji, T., Suzuki, H., 2003. Application of probe-vehicle data for real-time traffic-state estimation and short-term travel-time prediction on a freeway. Transportation Research Record: Journal of the Transportation Research Board 1855, 49–59.

National Highway Traffic Safety Administration, 2013. Preliminary statement of policy concerning automated vehicles. Press release.

Richards, P.I., 1956. Shock waves on the highway. Operations Research 4, 42–51.

Seo, T., Kusakabe, T., Asakura, Y., 2015. Estimation of flow and density using probe vehicles with spacing measurement equipment. Transportation Research Part C: Emerging Technologies 53, 134–150.

van Wageningen-Kessels, F., Yuan, Y., Hoogendoorn, S.P., van Lint, H., Vuik, K., 2013. Discontinuities in the Lagrangian formulation of the kinematic wave model. Transportation Research Part C: Emerging Technologies 34, 148–161.

Yuan, Y., van Lint, J.W.C., Wilson, R.E., van Wageningen-Kessels, F., Hoogendoorn, S.P., 2012. Real-time Lagrangian traffic state estimator for freeways. Intelligent Transportation Systems, IEEE Transactions on 13, 59–70.